Eddy covariance measurements of CO₂ exchange from agro-ecosystems located in subtropical (India) and boreal (Finland) climatic conditions

Pramit Kumar Deb Burman[1,2,*], Narasinha J Shurpali[3],
Subharthi Chowdhuri[4], Anandakumar Karipot[2], Supriyo Chakraborty[1,2],
Saara E Lind[3], Pertti J Martikainen[3], Seethala Chellappan[5],
Antti Arola[5], Yogesh K Tiwari[1], P Murugavel[4], Dinesh Gurnule[4],
Kiran Todekar[4] and Thara V Prabha[4]

[1]*Centre for Climate Change Research, Indian Institute of Tropical Meteorology, Pune 411 008, India.*
[2]*Department of Atmospheric and Space Sciences, Savitribai Phule Pune University, Pune 411 007, India.*
[3]*Department of Environmental and Biological Sciences, University of Eastern Finland, Yliopistonranta 1 E, P.O. Box 1627, 70211 Kuopio Campus, Finland.*
[4]*Cloud Aerosol Interaction and Precipitation Enhancement Experiment, Indian Institute of Tropical Meteorology, Pune 411 008, India.*
[5]*Finnish Meteorological Institute, P.O. Box 1627, 70211 Kuopio, Finland.*
Corresponding author. e-mail: pramit.cat@tropmet.res.in

Climate impacts agriculture in various complex ways at different levels and scales depending on the local natural crop growth limitations. Our objective in this study, therefore, is to understand how different is the atmosphere–biosphere exchange of CO_2 under contrasting subtropical and boreal agricultural (an oilseed crop and a bioenergy crop, respectively) climates. The oilseed crop in subtropical climate continued to uptake CO_2 from the atmosphere throughout the year, with maximum uptake occurring in the monsoon season, and drastically reduced uptake during drought. The boreal ecosystem, on the other hand, was a sustained, small source of CO_2 to the atmosphere during the snow-covered winter season. Higher rates of CO_2 uptake were observed owing to greater day-length in the growing season in the boreal ecosystem. The optimal temperature for photosynthesis by the subtropical ecosystem was close to the regional normal mean temperature. An enhanced photosynthetic response to the incident radiation was found for the boreal ecosystem implying the bioenergy crop to be more efficient than the oilseed crop in utilizing the available light. This comparison of the CO_2 exchange patterns will help strategising the carbon management under different climatic conditions.

Keywords. Carbon dioxide exchange; Eddy covariance; India; Subtropical climate; Sesame; Reed canary grass.

1. Introduction

Rising concentrations of greenhouse gases (GHG) in the atmosphere are a major driver of the global warming and climate change (Field *et al.* 2014).

Increasing anthropogenic activities including hike in fossil fuel consumption and land use are the key drivers for the growth of CO_2 in the atmosphere. For proper climate change mitigation measures, various sinks and sources of atmospheric CO_2 and

other GHGs need to be identified and their sink/source capacity needs to be quantified. Terrestrial ecosystems are the largest sink of atmospheric CO_2 with an estimated sink strength of $3.1 \pm 0.9 \, \text{GtC} \, \text{yr}^{-1}$ (Le Quéré *et al.* 2016). Over the years, land use conversion and agriculture have been an important source of GHGs to the atmosphere, responsible for about one-third of the global GHG emissions. However, such estimates are uncertain as available ground measurements for validation are sparse considering the diversity of biome types and climate zones spread across the globe.

The ecosystem–atmosphere carbon exchange is a complex biogeochemical process that depends on multiple factors such as the climate, plant functional type, availabilities of nutrients and water in the soil etc. (Ciais *et al.* 2013). For an accurate quantification of the carbon budget of any ecosystem, long-term monitoring of the biosphere–atmosphere exchange of scalars and energy along with governing ecophysiological variables is required (Baldocchi *et al.* 2001). Currently, the two most widely used techniques for measuring GHG exchange are the eddy covariance (EC) and closed chamber (manual or automated) methods. The EC method measures turbulent GHG fluxes for characterising flux dynamics at the landscape level (Baldocchi *et al.* 2001). Nowadays, the EC fluxes of CO_2 and water vapour are routinely measured across all the continents. A global network of EC stations called 'FLUXNET' links across a range of regional networks in North, Central and South America, Europe, Asia, Africa, and Australia (http://fluxnet.fluxdata.org). While this global network includes more than eight hundred active and historic flux measurement sites, spread across most of the world's climate space and representative biomes, the Indian subcontinent is thus far poorly represented in this network. The data on energy, mass, and momentum exchange from this region are urgently required for a better parameterization of the Earth System Models (ESMs), for example, for an improved understanding of the Indian southwest monsoon characteristics.

The South Asian carbon budget has a lot of uncertainty due to the scarcity of surface flux measurements over the Indian subcontinent (Patra *et al.* 2013). Several initiatives have been undertaken by the Indian Institute of Tropical Meteorology (IITM) (Deb Burman *et al.* 2017, 2019; Chatterjee *et al.* 2018; Sarma *et al.* 2018; Gnanamoorthy *et al.* 2019) and Indian Space Research Organisation (ISRO) (Watham *et al.*

2014) in this regard to establish EC towers over different ecosystems across the country for continuous monitoring of their long-term exchanges of scalar and energy with the atmosphere. However such studies reporting the long-term EC GHG fluxes from agricultural ecosystems are still limited in number and insufficient to represent the diverse agricultural landscapes of the country (Patel *et al.* 2011; Bhattacharyya *et al.* 2013a, b). Moreover, to the best of our knowledge, globally no carbon flux study has been reported over the sesame crop using the EC technique. This is an important oilseed crop cultivated over most of the Indian subcontinent and African continent (Nath *et al.* 2001; Boureima *et al.* 2012). Globally India ranks in the top in the agricultural area and yield of sesame production with a variety of cultivars produced in different agroecological zones spanning over multiple states (Bisht *et al.* 1998; Kumar and Sharma 2011). In 2006–07, the Indian sesame production stood at 0.63 m tonne, 18.8% of the global production cultivated over 1.9 m ha agricultural field (http://agriexchange.apeda.gov.in/Market%20Profile/MOA/Product/Sesame.pdf).

Understanding the carbon dynamics and its relation to the environmental factors in a cropping system, vital to the food security and national economy will be helpful to assess its carbon sequestration potential and to estimate the probable future effect of climate change on its productivity. Such data will pave the way for an accurate representation of the physical and biological processes in crop production models (Lal *et al.* 1998, 1999; Mall and Aggarwal 2002). In this paper, we intend to understand the net ecosystem CO_2 exchange by this crop grown under the subtropical conditions in India in contrast with the agricultural CO_2 exchange by a cropping system in the high latitude, boreal climate in Finland.

With forestry and agriculture as the backbone of the regional economy, the Nordic countries such as Finland, Denmark, Sweden and Estonia have focused on the perennial bioenergy crop production as a means of mitigation and adaption to climate change and renewable energy options (Shurpali *et al.* 2010; Mander *et al.* 2012; Järveoja *et al.* 2013; Karki *et al.* 2015). Different species of such crops have been grown on different types of soil under different management practices. Subsequently their carbon cycles have been studied for a precise assessment of their carbon neutrality to be further used as fuel (Shurpali *et al.* 2009). Access to the EC based long term data from a perennial bioenergy

crop cultivated in eastern Finland gives us an opportunity to compare and contrast the CO_2 exchange patterns from cropping systems adopted in diametrically opposite climatic conditions. The broad objectives of this paper are to compare the atmospheric CO_2 exchange dynamics of two different agro-ecosystems located in two different climatic regions—northern India and eastern Finland. In this study, we aim to characterise and quantify the net ecosystem CO_2 exchange (NEE) from an oil seed crop in India and a perennial bioenergy crop in Finland and investigate the factors governing their CO_2 exchange. To the best of our knowledge, this is the first study that reports the EC based agricultural CO_2 exchange from the Indian subcontinent in comparison with the agriculture under boreal climate.

2. Materials and methods

2.1 *Study sites*

The Indian study site at Barkachha (25.06° N, 82.59° E, 169 m AMSL (above the mean sea level)) is located in the south campus of Banaras Hindu University (BHU), in the outskirts of a small town named Mirzapur, roughly 90 km southwest of the Varanasi city in the state of Uttar Pradesh (figure 1a). It is characterised by a uniform topography with homogeneous grassland and kharif (monsoonal—June to September) crop of the sesame oilseed (*Sesamum indicum*). According to
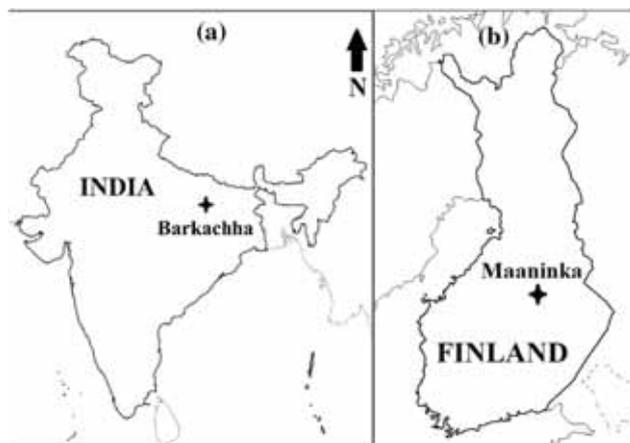

Figure 1. Study sites at (**a**) Barkachha (25.06° N, 82.59° E; 169 m AMSL), India and (**b**) Maaninka (63.16° N, 27.24° E; 89 m AMSL), Finland with their locations being marked by symbols on the corresponding country maps. AMSL refers to above the mean sea level.

the Köppen–Geiger climate classification, this region has a humid subtropical climate (Kottek *et al.* 2006). The surface weather station of the India Meteorological Department (IMD) nearest to Barkachha is located at Varanasi (25.30° N, 83.02° E). Climatological (30 years, reference period 1985–2015) mean annual air temperature (T_{air}) at Varanasi is 24.1°C; May and January are the hottest and coldest months with monthly mean T_{air} of 32 and 12°C, respectively (figure 2a). The annual precipitation in this region is 948 mm; August and December are the wettest and driest months with average total precipitation (precip) of 268 and 5 mm, respectively (figure 2b).

The observations made at the Barkaccha site and presented in this paper are part of an umbrella project entitled Cloud–Aerosol Interaction and Precipitation Enhancement Experiment (CAI-PEEX). This project is funded by the Ministry of Earth Sciences (MoES), the Government of India and implemented by the Indian Institute of Tropical Meteorology (IITM), Pune (Prabha *et al.* 2011; Deb Burman *et al.* 2018). As part of this project several micrometeorological instruments (described below) were deployed on a 20 m tall tower for collecting the surface layer observations from June 2014 to April 2016, over the Indo-Gangetic plain.

The study site at Maaninka located in eastern Finland (63.16° N, 27.24° E, 89 m AMSL) is a 6.3 ha agricultural field cultivated with the reed canary grass (RCG, hereafter; scientific name *Phalaris arundinacea* L., variety 'Palaton'), a perennial bioenergy crop. Boreal climate prevails in this region according to the Köppen–Geiger climate classification (Kottek *et al.* 2006). Climatologically (30 yrs, reference period 1981–2010), mean annual T_{air} in this region is 3.2°C; the coldest and warmest months of the year are February and July with a mean T_{air} of –10 and 17.0°C, respectively (Lind *et al.* 2016). On average, the total precipitation in a year in this region is 612 mm, with a part of the precipitation occurring as snow that begins to accumulate on the ground in October and stays until the end of April with an average maximum snow cover of 50 cm (Lind *et al.* 2016). July and April are the wettest and driest months at Maaninka with an average monthly total precipitation of 77 and 30 mm, respectively (figure 2d). Micrometeorological measurements carried out at Maaninka from July 2009 to December 2011 and published in Lind *et al.* (2016) are used in the present study.
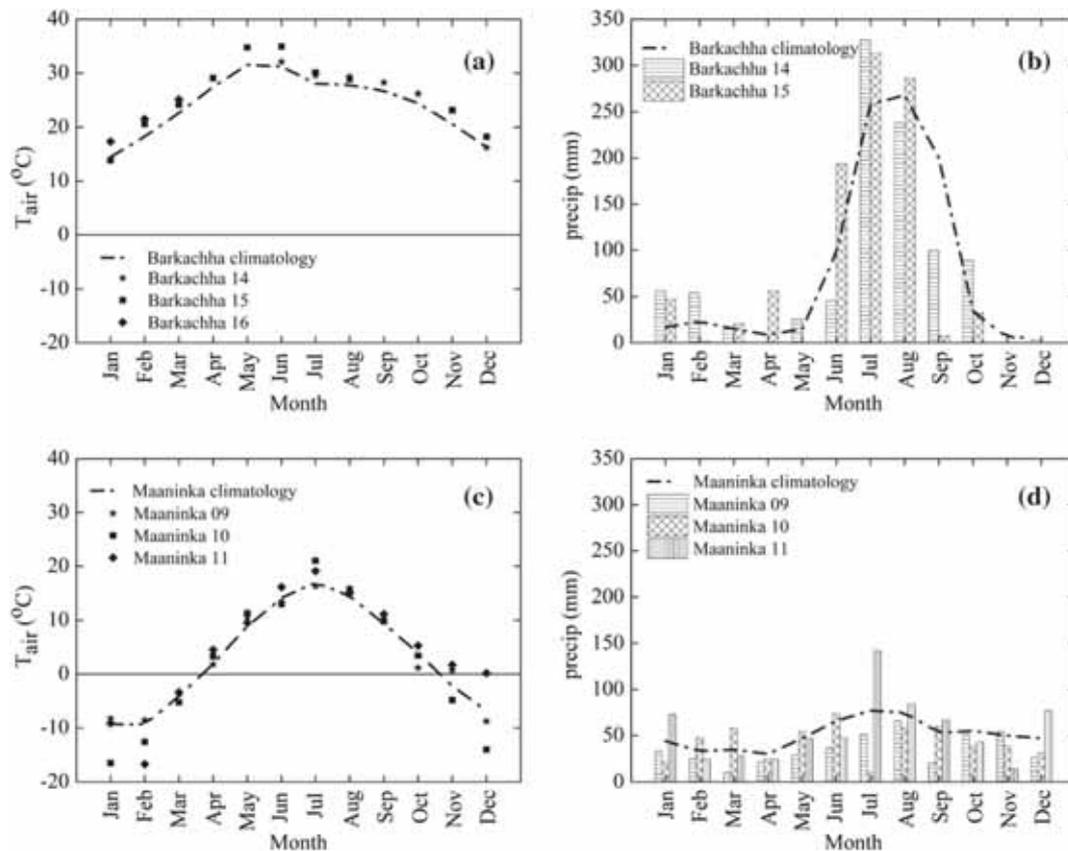
Figure 2. Climatological and measured monthly averaged (**a**) air temperature (T_{air} in °C), (**b**) precipitation (precip in mm) at Barkachha, (**c**) air temperature (T_{air} in °C) at Maaninka, and (**d**) precipitation (precip in mm) at Maaninka.

2.2 *Farming practises at Barkachha and Maaninka*

The agriculture in the Barkachha region is mostly rainfed and hence largely dependent on the Indian summer monsoon. The sesame crop is planted in July, at the beginning of monsoon over this region, and harvested in October. The land remains covered by the patches of grass with scattered, small shrubs during the rest of the year; no crop is grown during those months. Such type of agricultural practice is known as the 'Kharif cropping' in India.

The Maaninka study site was used for the cultivation of forage grasses, barley or oat until 2008. Since 2009, RCG, a perennial bioenergy crop with a rotation cycle of 10–15 yrs was cultivated at this site. Late sowing in June during the first year of crop establishment is a general practice for this crop and therefore, the perennial RCG crop was established in the early June of 2009. However, in subsequent years, the initial sprouting occurred soon after the air temperatures increased and snow melted by the end of April. The crop grew continuously for seven to nine weeks since the beginning of July in 2009 and from mid-May onwards in

2010 and 2011. Owing to a late start in 2009, the crop was primarily in vegetative growth with RCG plants thriving well with peak growth under cool weather prevailing during early October in that year. This is consistent with the fact that the crop allocates its carbon resources to the development of strong roots and rhizomes during the establishment year in a rotation cycle. In 2010 and 2011, however, the plants started flowering around the middle of June. Following the common agricultural practice in this region, crops were harvested in every spring following the second growing season (on April 28 in 2011 and May 9 in 2012). For Barkachha, we defined the period from June to October as the growing season and for Maaninka from May to September with the rest of the year defined as the non-growing season.

2.3 *Tower instrumentation*

The 20 m tall flux tower at Barkachha was equipped with an EC system installed at 5 m and consisted of a WindMaster Pro 3D sonic anemometer-thermometer (Gill Instruments,

Lymington, UK) and an open-path infrared CO_2–H_2O analyzer (IRGA) LI7500A (Li-COR Inc. Lincoln, Nebraska, USA). The EC system measured and recorded the zonal, meridional and vertical wind velocity components (u, v, and w in m s^{-1}), and the mixing ratios of CO_2 (c in μmol mol^{-1}), and water vapour (q in mmol $mole^{-1}$) at a sampling frequency of 10 Hz. Five sets of multi-component weather sensors WXT520 (Vaisala Oyj, Finland) measuring air temperature (T_{air}), pressure, relative humidity (RH), precipitation (precip), wind speed, and direction every minute were mounted at 3, 7, 12, 15, and 20 m. A four-component net radiometer CNR4 (Kipp and Zonen Inc., Delft, the Netherlands) was installed at 2.5 m to measure the incoming and outgoing components of net radiation (R_{SW}(in), R_{SW}(out), R_{LW}(in), and R_{LW}(out) in W m^{-2}) every minute. All supporting meteorological data were stored in a CR3000 data-logger (Campbell Scientific, Logan, Utah, USA). More details about the instrumentation of the Barkachha flux tower can be found in Sathyanadh *et al.* (2017). Vapour pressure deficit (VPD) has been calculated from T_{air} and RH. Climatological T_{air} and precip data were obtained from the IMD surface station at Varanasi.

The details of EC and supporting meteorological instrumentation at the Maaninka site are given in Lind *et al.* (2016). A measurement mast was installed at the Maaninka site with a variable measurement height, adjusted according to the growth of the vegetation. The EC instrumentation consisted of a R3-50 3D sonic anemometer (Gill Instruments, Lymington, UK) and an IRGA (closed-path LI7000 (primary) or LI6262 (backup); Li-COR Inc. Lincoln, Nebraska, USA), for measuring wind velocity components, sonic temperature, and gas concentrations, respectively. A weather station was set up close to the EC mast, height of which again varied along with the EC system, for measuring net radiation (CNR1; Kipp and Zonen Inc., Delft, the Netherlands), air temperature and relative humidity (HMP45C; Vaisala Oyj., Finland), photosynthetic photon flux density or PPFD (SKE211; Skye Instruments Ltd., Llandrindod Wells, UK), wind speed and direction (03002-5; R.M. Young Company, Michigan, USA), amount of rainfall at about 1 m height (52203, R.M. Young Company, Michigan, USA), and air pressure (CS106PTB110 Barometer; Vaisala Oyj., Finland). Data were stored in a CR3000 data-logger (Campbell Scientific Inc., Logan, Utah, USA).

2.4 *Satellite LAI data*

Leaf area index (LAI) is a biophysical parameter defined as the total single-sided leaf surface area per unit ground area (Watson 1947). It is an estimate of the leaf phenology, an important variable in explaining the photosynthetic and carbon sequestration capacity of any vegetated ecosystem. Moderate Resolution Imaging Spectroradiometer (MODIS) is a sensor onboard Terra and Aqua satellites by the National Aeronautics and Space Administration (NASA), USA for observing different biophysical parameters. In the present work, we have used the MCD15A3H product (MODIS/ Terra+Aqua Leaf Area Index 4-day L4 Global 500 m Sin Grid V006) downloaded from MODIS and VIIRS Land Products Global Subsetting and Visualization Tool. ORNL DAAC, Oak Ridge, Tennessee, USA (ORNL DAAC 2018) for studying the annual vegetation profile of the crops at Barkachha and Maaninka. For each of these sites, the quality-controlled average LAI values over an area of 0.25 km^2 representing the study sites have been used in our analysis (Myneni and Park 2015).

2.5 *Reanalysis data*

As the radiation measurement at Barkachha was not continued for the entire duration of flux tower campaign, we have used the MERRA-2 (Modern-Era Retrospective Analysis for Research and Applications, Version-2) reanalysis product (Gelaro *et al.* 2017) to obtain the incoming shortwave radiation (R_{SW}(in)) at hourly time-scale. Additionally, the photosynthetic photon flux density (PPFD) at Barkachha has been estimated at hourly time-scale from the R_{SW}(in) following Escobedo *et al.* (2009).

2.6 *Flux calculation and quality control*

We computed the CO_2 flux (NEE) for the Barkachha site from the EC measurements of w and c following the Reynolds averaging method (Aubinet *et al.* 1999) using the EddyPro software version 6.2.0 (https://www.licor.com). Several rigorous quality control measures were applied to the raw EC data prior to the flux calculation that includes the angle of attack correction (Nakai *et al.* 2006), depsiking (Mauder *et al.* 2013), block-averaged detrending, and first and second coordinate rotations (Kaimal and Finnigan 1994). The time

lag between the measured wind components and the mixing ratios (c and q) is compensated by a time lag correction (Burba 2013). We applied the WPL correction (Webb *et al.* 1980) to remove the effect of density perturbation of the air due to the moisture content. Random uncertainties due the flux sampling error are normalized following Webb *et al.* (1980). High (Moncrieff *et al.* 2004) and low-pass filters (Moncrieff *et al.* 1997) are applied for compensating the loss of fluxes at the low and high frequency ranges of the flux spectrum. Additionally a daily quality control file was generated along with the fluxes, containing statistical parameters and flags for stationarity and well developed turbulence tests for the calculated fluxes (Foken *et al.* 2004). We detected the outliers in the fluxes by the median absolute deviation (MAD) method and subsequently removed them following Papale *et al.* (2006). Data gaps occur in the long term continuous measurement of meteorological variables due to multiple reasons including sensor malfunctioning, adverse weather, power shortage, etc. Finally, we used the REddyProc (Wutzler *et al.* 2018), an open source R package developed by the Department of Biogeochemical Integration, Max Planck Institute of Biogeochemistry, Jena, Germany for filling the gaps in CO_2 flux data.

The CO_2 flux (NEE) at Maaninka was computed using the EddyUH software (http://www.atm.helsinki.fi/Eddy_Covariance/index.php) developed by the University of Helsinki, Finland (Mammarella *et al.* 2016). The data were despiked following a difference limit in the subsequent data points (15 µmol mol^{-1} for c and 20 mmol mol^{-1} for q) and replacing a 'spike' with the consecutive value. The data were coordinate rotated twice and block-averaged detrending was applied. The data were corrected for the lag time by maximising the covariance. The low and high frequency spectral corrections were implemented according to Rannik and Vesala (1999) and Aubinet *et al.* (1999), respectively. Following Schotanus *et al.* (1983) the effects of humidity on heat fluxes were corrected. The NEE was filtered using a u* filter of 0.1 m s^{-1}. The non-stationary fluxes were rejected according to Foken and Wichura (1996). Overall flags were defined according to Foken (2008); flags higher than or equal to 7 were removed. Finally, the data were visually inspected. The data were gap filled using the online facility available at http://www.bgc-jena.mpg.de/∼MDIwork/eddyproc/index.php (Reichstein *et al.* 2005). More details about these can be found in Lind *et al.* (2016). According to the convention we followed in this paper the negative and positive values of NEE signify uptake and release of CO_2 by the ecosystem, respectively.

2.7 *Supporting micrometeorological variables as drivers of the ecosystem–atmosphere CO_2 exchange*

The ecosystem–atmosphere exchange of CO_2 is a complex interplay of meteorology and plant physiology. Distinct climatic conditions exist at Barkachha and Maaninka during different times of the year. Additionally, the plants undergo different stages of their lifecycle during different times of the year. Combined together, these result in prominent seasonality in NEE at both these sites. To probe such seasonality, monthly averaged diurnal patterns of NEE at half-hourly time-scale were computed and studied for the representative months of the growing and non-growing seasons. At Barkachha the growing months include July and August of 2014 and 2015 and the non-growing months include December of 2014 and 2015 and January of 2015 and 2016. At Maaninka, the growing months are July and August of 2009, 2010, and 2011 and the non-growing months are December of 2009, 2010, and 2011 and January of 2010 and 2011.

Additionally, we studied the effects of T_{air}, VPD, and PPFD on NEE during the growing and non-growing seasons. For this purpose, we selected one month for each season and site. The selected growing and non-growing months at Barkachha are July of 2015 and January of 2016 respectively, and at Maaninka February and July of 2011, respectively. For all these months the dependencies of NEE on T_{air}, VPD, and PPFD are studied at hourly time-scale. Only the daytime (R_{SW}(in) > 20 W m^{-2}) values have been considered (Reichstein *et al.* 2005) for such analyses. For a better understanding of the relation between different variables, appropriate equations have been fit to their respective scatter plots and summarised in table 1.

A rectangular hyperbola model was fit to explain the relation between NEE and PPFD following the Michaelis–Menten equation using the non-linear regression technique. This equation (Wang *et al.* 2017) can be mathematically expressed as:

$$NEE = \frac{\alpha * NEE_{sat} * PPFD}{NEE_{sat} + \alpha * PPFD}. \qquad (1)$$

where α (in µmol CO_2 µmol^{-1} photons) is the initial slope of the NEE versus PPFD curve, defined as

Table 1. *Fit parameters and R^2 values for the relations between NEE and T_{air}, and NEE and VPD at Barkachha and Maaninka for the growing season. The equations used are $NEE = a_1 T_{air} + b_2 T_{air}^2 + c_1$ and $NEE = a_2 VPD + b_2 VPD^2 + c_2$ for Barkachha and $NEE = m_1 T_{air} + n_1$ and $NEE = m_2 VPD + n_2$ for Maaninka.*

Relations among variables	Barkachha	Maaninka
NEE versus T_{air}	$a_1 = 0.7$	$m_1 = -0.5$
	$b_1 = -42.5$	$n_1 = -0.1$
	$c_1 = 649.5$	$R^2 = 0.1$
	$R^2 = 0.3$	
NEE versus VPD	$a_2 = 0.05$	$m_2 = -1.0$
	$b_2 = -2.1$	$n_2 = -0.4$
	$c_2 = 8.35$	$R^2 = 0.3$
	$R^2 = 0.2$	

the quantum efficiency or yield, and NEE_{sat} is the NEE at the light saturation, i.e., infinitely large value of PPFD, also known as the photosynthetic saturation.

3. Results and discussions

The two research sites considered in this study are poles apart in their soil, vegetation, climatic and hydrological regimes. Barkaccha is located in the central Vindhyan plateau region with a semi-arid to sub-humid climate. Rainfed agriculture is the traditional farming practice followed in the region with a variety of agricultural and horticultural crops, medicinal and aromatic plants being the main products. Red lateritic soils of this region are considered to be of low fertility (Kashiwar *et al.* 2018). On the other hand, Maaninka, situated in the North Savo region, located in the middle-eastern part of Finland, is specialised in the dairy milk and beef production. The agriculture in the region is limited by the short growing seasons and low growing degree days during the cropping season. The soils in this region are medium textured regosols with higher soil organic matter content than Barkaccha. Such regional differences influenced the CO_2 exchange patterns of the different agricultural cropping systems adopted in these two regions.

3.1 *Climatic conditions*

Based on the monthly climate statistics (figure 2), the annual range of T_{air} variation is 20°C at Barkachha, which is smaller than the 27°C annual T_{air} variation at Maaninka. Sub-zero condition persists for five months in a year at Maaninka, whereas it is

never the case at Barkachha. As we see from these observations, being located in the boreal region, Maaninka experiences more severe climatic variations throughout the year than Barkachha that is situated in the subtropical region and thus experiences a much moderate climate. Additionally, with a cumulative annual precipitation of 948 mm, Barkachha receives almost 50% more rainfall than Maaninka that has a cumulative annual precipitation of 612 mm. Most of the rainfall at Barkachha occurs during June to September brought in by the Indian summer monsoon. Although Barkaccha receives about 948 mm rainfall annually, it is far less than the Penman–Monteith potential evapotranspiration estimates of about 1551 mm per year (Ramarao *et al.* 2018). Hence a simple water balance calculation suggests this region to have a water deficit of about 600 mm per year and is often classified as arid (Matin and Behera 2017).

The study period at Barkachha was warmer than the 30-year average climate. The cumulative annual precipitation at Barkachha was 953 mm in 2014 and 957 mm in 2015, both marginally higher than the climatological mean; precipitation was maximum in July at 328 and 286 mm, in 2014 and 2015 respectively; in both these years November and December were the driest months with no precipitation.

At Maaninka, the summer months of measurement, i.e., May, June, and July were hotter than the average, and winter months, i.e., January and February were colder with the exception of 2011 when November and December were warmer than normal. Cumulative annual precipitation at Maaninka was 421, 512, and 670 mm in 2009, 2010, and 2011 respectively; August, June, and July were the wettest months in 2009, 2010, and 2011, respectively with precip being 66, 74, and 142 mm, correspondingly. March, June, and November were the driest months at Maaninka in 2009, 2010, and 2011 respectively with precipitation not exceeding 10 mm. Maaninka receives about 600 mm precipitation annually, together as snow during the winter and rain during the summer months. Water balance studies for Finland have shown that the boreal region experiences a surplus of water on an annual basis (Solantie 2006).

3.2 *Annual patterns of vegetation growth*

The annual LAI patterns at Barkachha and Manninka during the corresponding measurement periods are plotted in figure 3. Overall at
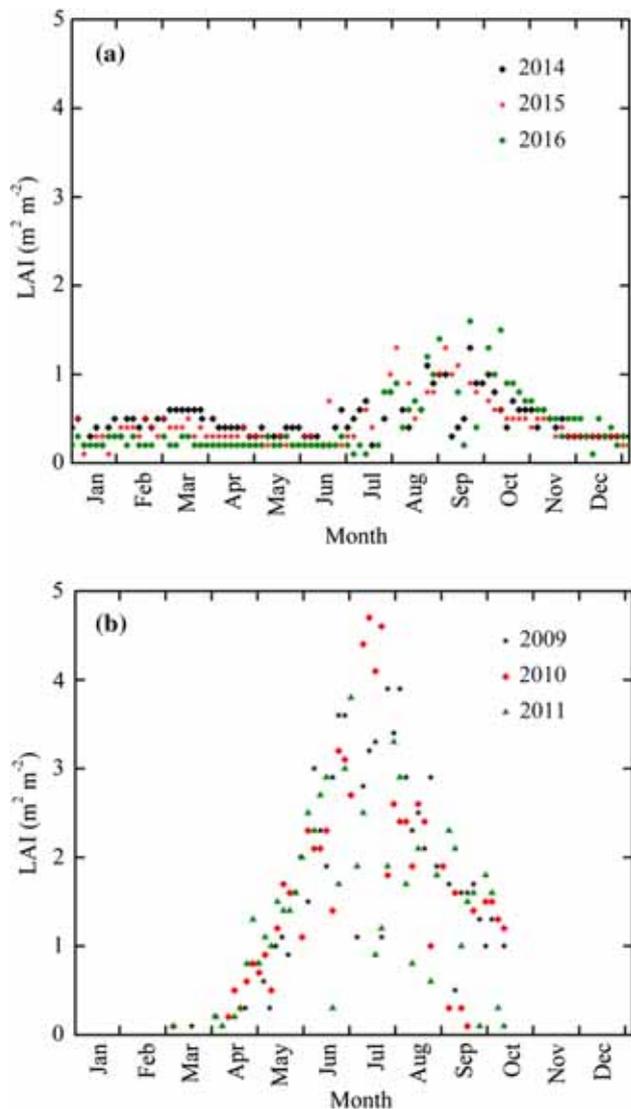
Figure 3. MODIS-derived leaf area index (LAI in $m^{-2} m^{-2}$) at (**a**) Barkachha during 2014–2016 and (**b**) Maaninka during 2009 to 2011 at 4-day temporal resolution.

Barkachha, the canopy growth is maximum during the monsoon (July to September) contributed by the sesame crop grown around this season following the Kharif cropping practice explained in section 2.2 and minimum during the rest of the year indicative of the scattered growths of grass and shrubs around this time (figure 3a). Among the measurement years the maximum LAI varies between 1.5 and 2 $m^2 m^{-2}$, whereas the minimum LAI ranges within 0.25–0.5 $m^2 m^{-2}$, during the rest of the year (figure 3a).

At Maaninka, during the winter months sub-zero condition prevails (figure 2c) and the ground remains snow-covered, devoid of any vegetation as reflected in the nil LAI values during this season (figure 3b). April onwards the LAI increases

gradually and reaches maximum in July (figure 3b) which is also the climatologically warmest month in this region (figure 2c). The maximum LAI varies between 3 and 5 $m^2 m^{-2}$ among the years in coherence with the crop growth as described in section 2.2. Among the measurement years the LAI is maximum at 4.75 $m^2 m^{-2}$ in 2010 when the RCG crop matured (figure 2c). The LAI is smaller in 2009 and 2011 when the crop was planted and harvested, respectively. Growing season LAI is larger at Maaninka in comparison with Barkachha (figure 3) resulting from a larger uptake of carbon as described next in this paper.

3.3 *Net ecosystem CO_2 exchange*

The half-hourly NEE data measured at Barkachha and Maaninka during the respective study periods are plotted together in figure 4. These values are quality controlled, but not gap-filled. At both the sites, stronger and weaker uptakes are seen during the growing and non-growing seasons, respectively. Additionally, the respiratory loss of CO_2 is also higher in the growing seasons at both the sites. In the growing season of 2014, the amplitude of NEE varies between –20 and 8 μmol $m^{-2} s^{-1}$ at Barkachha. This variation of amplitude gets smaller (between 0 and 5 μmol $m^{-2} s^{-1}$) in the corresponding non-growing season. Compared to 2014, the amplitude of variation is stronger in the growing season of 2015 with an uptake of –25 μmol $m^{-2} s^{-1}$ to and an ecosystem loss of 10 μmol $m^{-2} s^{-1}$. In the non-growing season of 2015, NEE varies between –5 and 2.5 μmol $m^{-2} s^{-1}$. This stronger carbon assimilation is translated into a fuller growth of canopy and reflected in a larger LAI during the growing season in 2015 compared to 2014 at Barkachha (figure 3a).

At Maaninka, prominent inter-annual variation in the uptake and release of CO_2 is visible in the growing as well as the non-growing seasons due to the different stages of growth of crop canopy. Growing season NEE varied between –25 and 15 μmol $m^{-2} s^{-1}$ in 2009, –30 to 15 μmol $m^{-2} s^{-1}$ in 2010, and –35 to 15 μmol $m^{-2} s^{-1}$ in 2011. Clearly, owing to enhanced photosynthetic capability, the vegetation absorbed more CO_2 from the atmosphere when the vegetative growth was at its peak as supported by the LAI record (figure 3b). Additionally, the respiration also increased, coincident with the high rates of release from the ecosystem to the atmosphere. However, as the rate of uptake was higher than loss, overall the ecosystem absorbed
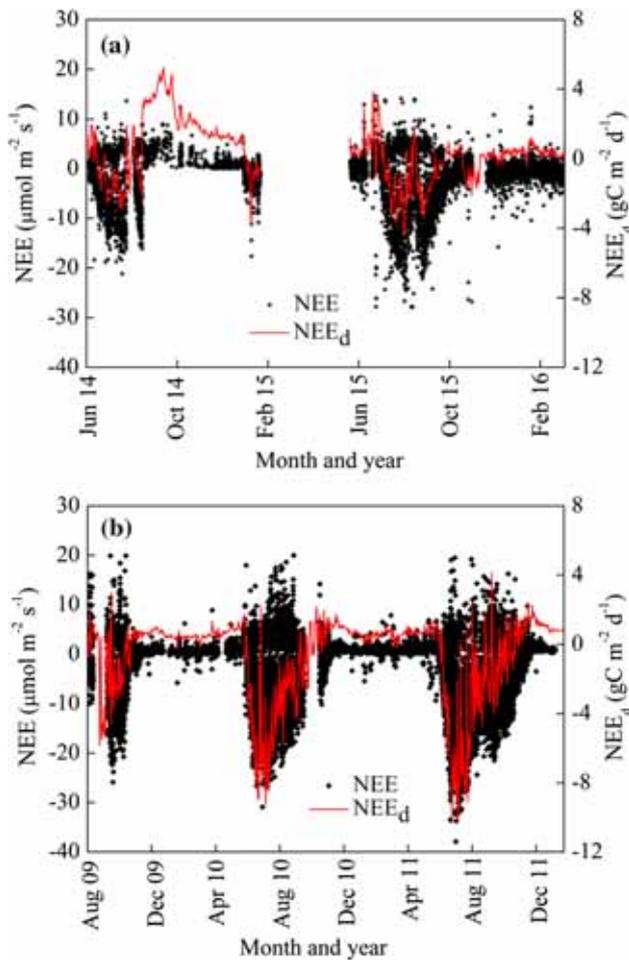
Figure 4. Calculated half-hourly and daily net ecosystem exchanges NEE (in µmol m^{-2} s^{-1} and NEE$_d$ in gC m^{-2} d^{-1}, respectively) at (**a**) Barkachha during June 2014 to July 2016 and (**b**) Maaninka during July 2009 to December 2011.

more atmospheric CO_2. There was not much inter-annual variation among the non-growing seasons at Maaninka as the vegetation was dormant owing to low temperatures and the ground being covered with snow. A small but positive NEE was maintained at these times.

The daily sums of quality controlled and gap-filled NEE (NEE$_d$ in gC m^{-2} d^{-1}) for the entire duration of measurements at Barkachha and Maaninka are also plotted in figure 4. In 2014, the ecosystem at Barkachha sequesters carbon in growing season, i.e., during June to August as the NEE$_d$ is negative throughout these months (figure 4a). The maximum daily uptake during this year is –3 gC m^{-2} d^{-1}, observed in July. The ecosystem switches to be a source of carbon by the beginning of September and continues to be so till the end of the year. On a daily scale, the maximum loss of CO_2 occurs during September when NEE$_d$ is about 6 gC m^{-2} d^{-1}. The release of CO_2 by the

ecosystem decreases sharply from October onwards. As indicated above, net daily uptake is seen in the non-growing month of January 2015 as well when NEE$_d$ remains negative (as high as –4 gC m^{-2} d^{-1}). This happens probably due to high available soil moisture (50 mm accumulated rainfall in this month which is twice the climatological mean rainfall January, figure 2b). During June to December 2014, the cumulative loss of carbon (NEE) by this ecosystem was 235 gC m^{-2}.

Unlike 2014, the ecosystem at Barkachha remains a source of CO_2 in the month of June in 2015 (figure 4a). The magnitude of maximum release of CO_2 in this month is 4 gC m^{-2} d^{-1}. Subsequently, from July onwards, the ecosystem starts taking up carbon. A maximum uptake of –5 gC m^{-2} d^{-1} is seen in August this year. Apart from a few isolated days in this month when NEE$_d$ is positive, the Barkachha ecosystem remains a carbon sink until October. The cumulative growing season NEE in 2015, i.e., the net carbon fixed by the Barkachha ecosystem from June to September in this year is 90 gC m^{-2}. Surprisingly, the ecosystem appears to take up CO_2 (about –2 gC m^{-2} d^{-1}) even in the month of November. The Barkachha ecosystem remains a source of CO_2 with an average NEE of 1 gC m^{-2} d^{-1} from December 2015 till the end of March 2016 when the measurement at Barkachha ended. This subsequently reduces the cumulative NEE of the Barkachha ecosystem to –60 gC m^{-2} in the longest available stretch of measurement, i.e., during June 2015 to February 2016. Additionally, the cumulative uptake by the Barkachha ecosystem in the January and February 2015 stands at another 31 gC m^{-2}. However, the annual total NEE at Barkachha could not be computed due to no measurements in the pre-monsoon seasons (March–April–May) of 2014 and 2015. As the pre-monsoon or spring is conducive for plant growth, the net annual carbon exchange cannot be calculated without taking this period into account.

During 2014, Barkachha ecosystem sequestered atmospheric CO_2 from May until August. However, CO_2 sink activity during 2015 lasted from July to October, although the total duration of CO_2 sink activity remains the same (four months) in both the years. Peak rate of CO_2 uptake is higher in 2015 compared to the previous year. The month of June was warmer than normal at Barkachha in 2015 (figure 2a). Such heat stress rendered the Barkachha ecosystem a source of CO_2 in June 2015, whereas in June 2014 it acted as a sink

owing to moderate conditions. The rainfall at Barkachha in September 2014 and 2015 was less than normal (figure 2b). Such dry conditions might have affected its carbon sequestering activity in these two months (Ciais *et al.* 2005). The Barkachha ecosystem received less than normal rainfall in the growing season of 2014 except July (figure 2b); the cumulative monthly deficit in rainfall was 60 mm in June, 35 mm in August, and 125 mm in September. Overall the rainfall deficit for this region (east Uttar Pradesh) was 42%. At the country scale this year was declared a deficit monsoon or drought year and the yield of the rainfed (Kharif) crops was severely affected (Pai and Bhan 2014; Mishra *et al.* 2016). The effect of such a severe water stress is evident in the presented data on the CO_2 exchange patterns of this rainfed ecosystem.

At the beginning of measurement in July 2009, the ecosystem at Maaninka briefly acts as a source of atmospheric CO_2 when an average release of 1 gC m^{-2} d^{-1} is recorded (figure 4b). However, it quickly transforms into a net sink and registers maximum uptake of –6 gC m^{-2} d^{-1} by the beginning of August. Subsequently, the NEE$_d$ decreases gradually but remains negative. The Manninka ecosystem remains a source from October 2009 to April 2010 with an average NEE of 1.5 gC m^{-2} d^{-1}. In the following year, the ecosystem undergoes a sharp transition to a sink in May. This is in advance compared to 2009 when the source to sink transition happens two months later in July. The peak NEE is larger at –9 gC m^{-2} d^{-1} in June 2010 compared to –6 gC m^{-2} d^{-1} in August 2009. The net uptake at Maaninka decreases gradually till the beginning of October in 2010 when the ecosystem switches over as a source. The maximum value of NEE$_d$ observed in October 2010 is 2 gC m^{-2} d^{-1}. From this time until May 2011, the Maaninka ecosystem continues to act as a source of atmospheric CO_2 with an average CO_2 loss rate of 1.5 gC m^{-2} d^{-1}. Again the source to sink transition takes place in the beginning of May in 2011. The highest net uptake of –10 gC m^{-2} d^{-1} among all the years is observed in 2011 at the beginning of August after which NEE continues to decline until the end of October 2011. However, on several isolated days during this period, NEE$_d$ is positive implying that the ecosystem acts as a source. From October 2011 to the beginning of February 2011 when the measurement is discontinued the Maaninka ecosystem acts as a source with a mean loss of 1.5 gC m^{-2} d^{-1}. The cumulative uptake by this

ecosystem is 56.7, 262 and 256 gC m^{-2}, respectively in 2009 (measurement period only), 2010 and 2011 (Lind *et al.* 2016).

The daytime uptake of CO_2 is stronger at Maaninka than at Barkachha during the growing season (figure 4). Additionally, the day-length is longer at Maaninka extending from 0400 to 2000 LT (local time) compared to 0600–1800 LT at Barkachha. As a result, plants are photosynthetically active for a longer duration in the day at Maaninka during the growing season. On the other hand, such increased growth results in more maintenance respiration by the plants. This is manifested in the stronger night-time release of CO_2 at Maaninka compared to Barkachha. However, averaged over a daily scale, the ecosystem sequesters more CO_2 at Maaninka than at Barkachha during the growing season. On the contrary, the ecosystem at Barkachha continues to sequester CO_2 at daytime during the non-growing season as well, although at low rates, while the Maaninka ecosystem acts as a weak, but constant source of CO_2 without any diurnal variation. These are reflected as small but finite LAI values at Barkachha but nil LAI at Maaninka during the non-growing season (figure 3).

3.4 *Mean monthly diurnal patterns of CO_2 exchange during growing and non-growing seasons*

The difference in vegetation cover during different times of the year (figure 3) brings in the seasonality in the ecosystem–atmosphere CO_2 exchange both at Barkachha and Maaninka (figure 5). The maximum uptake is observed at Barkachha during the daytime in the growing season (July and August), with the peak NEE being approximately –10 μmol m^{-2} s^{-1} in July 2014 and 2015 and –12 μmol m^{-2} s^{-1} in August 2015, respectively. During night, the respiration remains almost constant at 4 μmol m^{-2} s^{-1} (figure 5a). The strong sink activity of the ecosystem observed during the growing season is drastically reduced during the non-growing season (December and January). Nevertheless, a small uptake of –3 μmol m^{-2} s^{-1} is seen in the daytime; the respiration also reduces to 2 μmol m^{-2} s^{-1} at the night-time (figure 5b). Among the growing season months considered in this work at Barkachha, the daytime uptake is maximum at –14 μmol m^{-2} s^{-1} in August 2015. This is due to fact that the Barkachha ecosystem received above-normal rainfall ($\approx$ 280 mm) in this month (figure 5b).
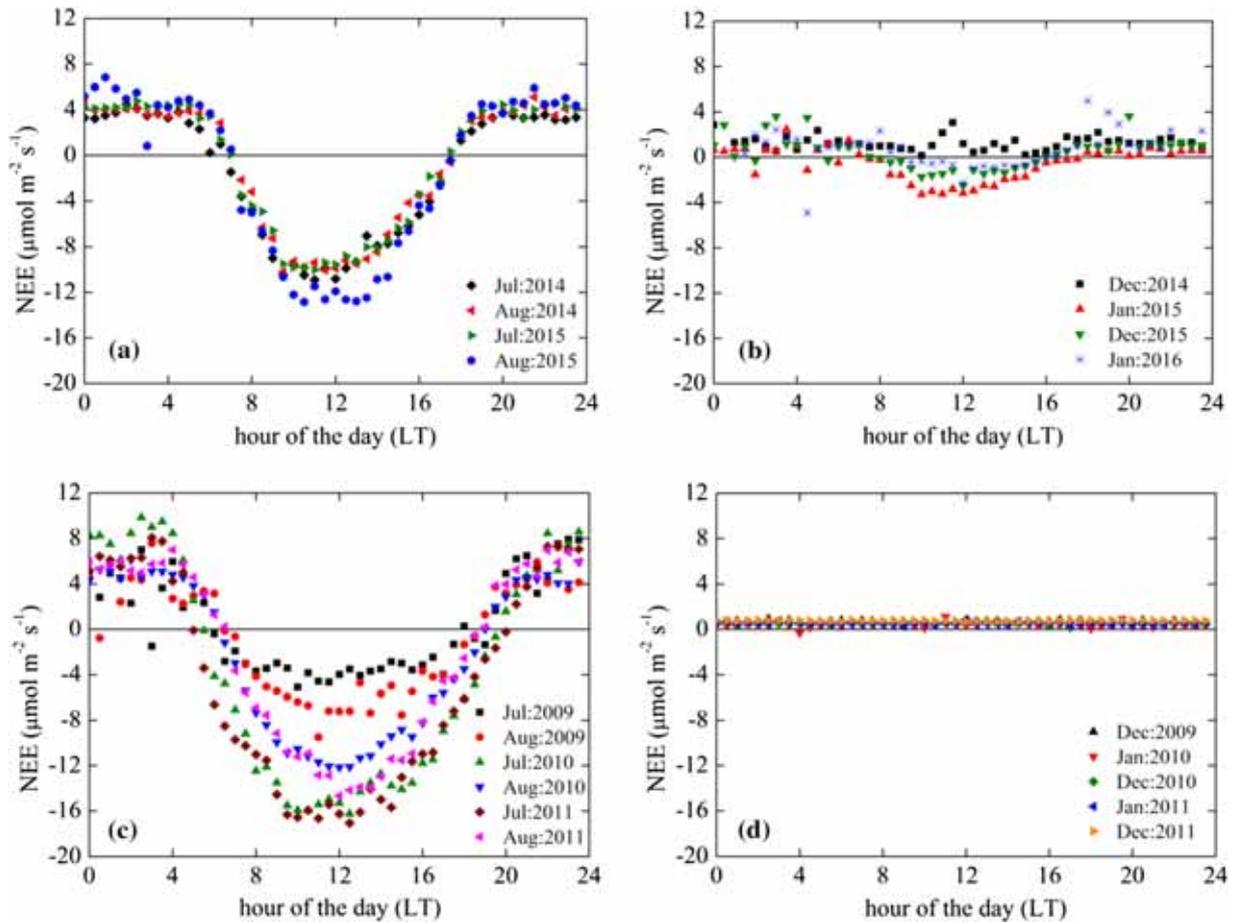
Figure 5. Monthly averaged diurnal variations of NEE (in μmol m^{-2} s^{-1}) with half-hourly resolution at (**a**) Barkachha during the growing season (July and August), (**b**) Barkachha during the non-growing season (December and January), (**c**) Maaninka during the growing season (July and August), and (**d**) Maaninka during the non-growing season (December and January) for the corresponding measurement periods (2009–2011 at Barkachha and 2009–2011 at Maaninka).

At Maaninka, the daytime uptake of CO_2 is stronger than the night-time release during the growing season (July and August) (figure 5c). However, the peak NEE increases with the maturity of RCG plants, i.e., the daytime uptake is maximum in 2010 when the RCG crops were fully matured compared to 2009 when they were sown and 2011 when they were harvested. The maximum and minimum uptakes are –18 and –4 μmol m^{-2} s^{-1}, observed in July during 2009 and 2011, respectively (figure 5c). Annually, the uptake is strongest in July. On a diurnal scale the ecosystem continues to act as a sink although the uptake reduces in August. The night-time respiration is high at 6 μmol m^{-2} s^{-1}, on average in the growing season. However, it varies in the range of 4–8 μmol m^{-2} s^{-1}. The NEE is near-zero but positive during the entire non-growing season (December and January) (figure 5d).

The day-length at Barkaccha varies from 10.5 hrs during winter to about 14 hrs during summer. On the contrary, the day-length at Maaninka varies from mere 4 hrs during December to nearly 21 hrs during June. Since the incident, photosynethetically active radiation is a major factor governing the CO_2 exchange of a vegetated surface; such wide variation in the day-length (2.5 hrs between winter and summer at Barkaccha as opposed to a staggering amplitude of 17 hrs at Maaninka) does have an impact on the CO_2 uptake by the crops. As the data presented here show, the seasonal sesame crop cultivated at Barkachha continues its photosynthetic activity during the growing season. During the rest of the year, the naturally growing grass and trees scattered over the study region contribute to the carbon uptake. As a result, an uptake is observed by the ecosystem even in the winter (non-growing) season. This is unlikely at Maaninka where the ecosystem acts as a sustained, weak source of carbon at daily scale in winter; no uptake even in the daytime can be seen. However, the net uptake seen at Barkachha is

lower during the non-growing season compared to the active growing season. On a daily scale, this helps offset the carbon loss by the ecosystem at the night-time. While in the growing season, the day-time uptake is higher in magnitude and renders the ecosystem as net sink of carbon at daily scale.

3.5 Climatic controls on the ecosystem–atmosphere CO_2 exchange

The daytime T_{air} has markedly stronger control over the daytime NEE during the growing season compared to the non-growing season, at both Barkachha and Maaninka (figure 6). The NEE does not change with increasing T_{air} during January 2016. However even in the non-growing season, the Barkachha ecosystem takes up CO_2, in the daytime (figure 6a). Such daytime uptake values in the non-growing season are mostly limited to –3 μmol m^{-2} s^{-1}, although at several instances when T_{air} is more than 20°C, sporadic uptake events as strong as –8 μmol m^{-2} s^{-1} do occur during the non-growing season at Barkaccha. During July 2015, the variation of NEE with T_{air} is much more prominent. Initially, NEE becomes more negative with increasing T_{air}, implying more uptake in the warmer environment. Maximum uptake of –20 μmol m^{-2} s^{-1} is observed when T_{air} is approximately equal to 31°C. Further increment in T_{air} gradually saturates and finally reduces the uptake. Eventually, positive NEE as small as 3 μmol m^{-2} s^{-1} is seen when T_{air} is around 34°C (figure 6a). Existence of such a 'critical T_{air}' for NEE is reported for different ecosystems by many researchers and a quadratic relationship between NEE and T_{air} (NEE = $a_1 T_{air}^2 + b_1 T_{air} + c_1$) is often found to best describe such a relation (Gu *et al.* 2005; Wang *et al.* 2017). The best fit quadratic relationship between the NEE and T_{air} is given in table 1.

The daytime T_{air} in February 2011 at Maaninka never exceeds 0°C. No uptake is seen in such cold environment. The NEE almost remains constant at 2 μmol m^{-2} s^{-1} throughout this month. In July 2011, CO_2 uptake increases with increasing T_{air}. However, there is a lot of scatter in the data implying the influence of other variables on the uptake process (figure 6b). Mean maximum uptake registered in this month is –23 μmol m^{-2} s^{-1}. In the growing season at Maaninka, the NEE increases in a linear fashion with the T_{air} (figure 6b). Unlike at Barkaccha the photosynthetic uptake neither

saturates nor decreases with an increasing T_{air}. Details of the linear fit (NEE = $m_1 T_{air} + n_1$) can be found in table 1.

The daytime VPD variation is stronger at Barkachha compared to Maaninka in both the growing and non-growing seasons (figure 6). While the maximum VPD registered in the growing season at Barkachha is around 30 hPa (figure 6c), the maximum VPD observed during the same season at Maaninka is < 25 hPa (figure 6d). Hence, the environmental moisture stress during the growing season at Barkachha is larger than Maaninka (Restaino *et al.* 2016). The VPD variation at Barkachha is similar in the growing and non-growing seasons, while at Maaninka the VPD variation is much stronger in the growing season. In the non-growing season, the VPD is negligibly small at Maaninka.

The non-growing season NEE is almost independent of the VPD at Barkachha, whereas in the growing season the NEE initially grows and subsequently decreases with VPD exceeding 20 hPa. To quantify the dependence of NEE on VPD behaviour a quadratic relationship (NEE = a_2VPD^2 + b_2VPD + c_2) was fit (table 1) following Wang *et al.* (2017). In the growing season at Maaninka, the photosynthetic uptake of CO_2 gradually increases up to –20 μmol m^{-2} s^{-1} till VPD reaches 15 hPa (figure 5d). A linear dependence on VPD (NEE = m_2VPD + n_2) best explains such behaviour of NEE with VPD (table 1) and is typical of several ecosystems (Lasslop *et al.* 2010; Wagle and Kakani 2014). A further increase in VPD saturates the uptake. A very small decreasing trend in the NEE is observed with VPD increasing beyond 20 hPa.

Light (PPFD) is a major driver of photosynthesis. Controls of daytime PPFD on the uptake at Barkachha and Maaninka during the growing and non-growing seasons are plotted in figure 6(e and f). In general, available light level is more at Barkachha compared to Maaninka in both the growing and non-growing seasons. The maximum PPFD at Barkachha during July 2015 and Maaninka during July 2011 are approximately 2000 and 1500 μmol m^{-2} s^{-1}, respectively. This is expected as being located in the subtropical belt Barkachha receives more PPFD than Maaninka which is located in the boreal region (Pinker and Laszlo 1992). The PPFD exerts much stronger control on the uptake during the growing seasons at both the sites.

The maximum PPFD is <1500 μmol m^{-2} s^{-1} at Barkachha in January 2016. The NEE does not vary significantly with the PPFD in this month

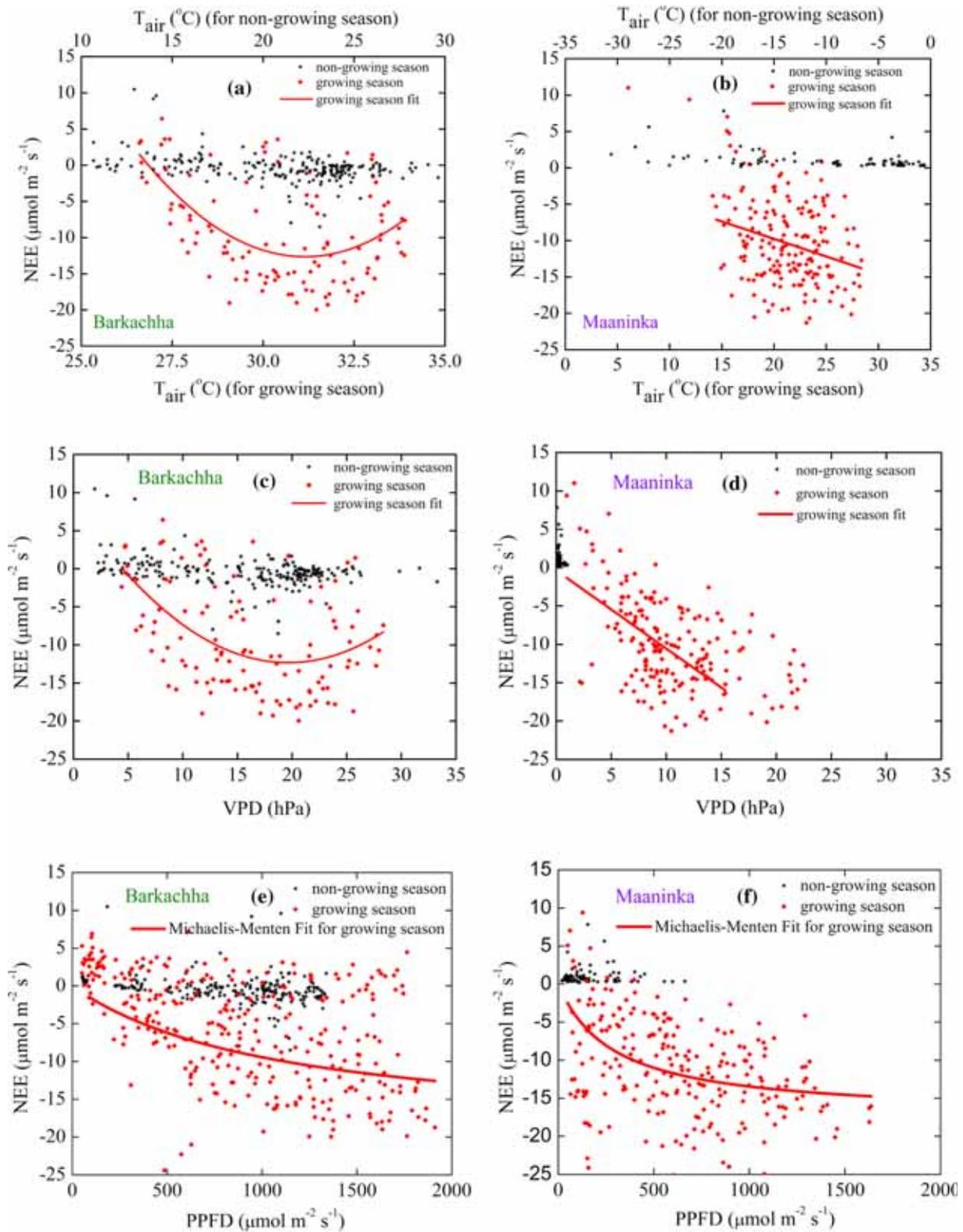Figure 6. Controls of T_{air} (in °C), VPD (in hPa), and PPFD (in µmol m^{-2} s^{-1}) on NEE (in µmol m^{-2} s^{-1}) at hourly time-scale during growing and non-growing months at Barkachha and Maaninka; (**a**) NEE vs. T_{air} for January 2016 and July 2015 at Barkachha, (**b**) NEE vs. T_{air} for February 2011 and July 2011 at Maaninka, (**c**) NEE vs. VPD for January 2016 and July 2015 at Barkachha, (**d**) NEE vs. VPD for February 2011 and July 2011 at Maaninka, (**e**) NEE vs. PPFD for January 2016 and July 2015 at Barkachha, and (f) NEE vs. PPFD for February 2011 and July 2011 at Maaninka. Additionally, in (**e**) and (**f**) Michaelis–Menten relations are fit between NEE and PPFD during the growing months using the non-linear regression NEE = α.NEE$_{max}$.PPFD/(NEE$_{max}$ + α.PPFD) (equation 1). Only measured data are used in the analysis.

(figure 6e). In July 2015, at Barkachha, the NEE increases gradually with the PPFD in a non-linear fashion. The rate of increase of NEE with PPFD decreases with the increasing PPFD. In July 2011, at Maaninka, a similar non-linear response of NEE to PPFD is observed. There is a strong sign of the possible saturation of NEE at the larger values of PPFD at Maanika in July 2011. However, such an indication of the possible saturation of NEE with PPFD is rather weak at Barkachha. The quantum efficiency, α is –0.019 and –0.057 μmol CO_2 μmol^{-1} photons in the growing seasons at Barkachha and Maaninka, respectively. The photosynthetic saturation, NEE_{sat} is –19.8 and –17.3 μmol m^{-2} s^{-1} correspondingly.

The critical or optimal T_{air} for photosynthesis by the Barkachha ecosystem is 31°C in the growing season (figure 6). This is the same as the climatological mean growing season T_{air} at Barkachha (figure 2a) showing the adaptation of the ecosystem to the ambient environment for maximum productivity. Over a lowland flooded rice ecosystem in India, such an optimal T_{air} was found to be 34°C (Bhattacharyya *et al.* 2013a). According to Huxman *et al.* (2003), the initial increase in uptake with T_{air} is due to the enhanced photosynthesis whereas, the later reduction in NEE can be attributed to the enhanced CO_2 emission from soil at higher T_{air}. Additionally the elevated radiation load on the plants at the higher T_{air} values can also decrease their photosynthetic activity (Fu *et al.* 2006).

The increasing VPD signifies growing moisture deficit in the atmosphere that results in the increased transpiration by plants. The transpiration and photosynthesis are two closely coupled processes regulated by stomata (Wang and Dickinson 2012). Hence, the enhanced transpiration under optimum soil moisture conditions results in enhanced photosynthesis and CO_2 uptake. Thus NEE initially increases with increasing VPD at Barkachha in the growing season (figure 6c). However, a further increase in VPD results in a greater water loss by transpiration from the plants. To prevent this, the stomata are closed and photosynthesis in turngets restricted (McCaughey *et al.* 2006). This is reflected in reduced uptake in July 2015 at Barkachha when VPD exceeds 20 hPa (figure 6c).

The quantum efficiency, α is –0.02 and –0.06 μmol CO_2 μmol^{-1} photon in the growing seasons at Barkachha and Maaninka, respectively. The photosynthetic saturation, NEE_{sat}, is –19.8 and –17.3

μmol m^{-2} s^{-1} correspondingly. In an earlier study, α has been reported to be –0.02 μmol CO_2 μmol^{-1} photons for a matured wheat canopy at Meerut in Uttar Pradesh, India (Patel *et al.* 2011). Additionally, α was found to be –0.035 and –0.042 μmol CO_2 μmol^{-1} photons for the month of July respectively at a mangrove (Rodda *et al.* 2016) and a mixed deciduous forest (Watham *et al.* 2014) over India. For an RCG cultivation in Denmark, α was reported to vary widely between –0.041 and –0.064 μmol CO_2 μmol^{-1} photons depending on the harvesting practice and fertilizer application (Kandel *et al.* 2016).

The α in the growing season at Maaninka is three times larger than Barkachha which signifies that the photosynthesis increases at a much faster rate at the Maaninka ecosystem. On the other hand, the NEE_{sat} is larger at Barkachha than Maaninka. It emphasizes that the true potential of photosynthesis by the plants in Barkachha ecosystem is higher than the actual peak photosynthesis observed at this site. However, the full potential of photosynthesis is not completely realised owing to severe climatic stress under high temperature conditions. This is evident in the relation of NEE with T_{air} and VPD. The NEE at Barkaccha increases with increasing temperature and VPD until an optimum temperature. With further increase in T_{air} and VPD beyond a threshold, maintaining a proper plant water status becomes the priority. This leads to a closure of the sesame stomata and thus a reduction in the net uptake of CO_2 by the crop.

The RCG crop at Maaninka sequesters less carbon during its initial growth in 2009. Once fully matured, it sequesters more carbon, as observed during the 2010 and 2011 growing seasons (Lind *et al.* 2016). The ecosystems native to boreal regions are acclimatised to perform under short growing seasons. The RCG crop, planted at Maaninka, responds effectively to increasing day length with a high value of α. Moreover, the estimated NEE_{sat} for Maaninka is slightly lower than the NEE_{sat} estimated for Barkachha. Owing to longer day-length, moderate temperatures and high evaporative demand, optimum soil moisture and timely supply of NPK (Nitrogen–Phosphorus–Potassium) and micro nutrients, the crop sequesters more carbon at a daily scale in the growing season.

Despite having a higher NEE_{sat}, the sesame crop at Barkaccha fails to tap its true potential of photosynthesis, even during the growing season. It is evident by the large value of NEE_{sat} and comparatively lower value of actual, peak uptake. Additionally, a low value

of α during the growing season at Barkachha signifies that the rate of photosynthesis is slow compared to the potentially conducive conditions offering plenty of light and high temperatures. This suggests indirectly that soil water status and nutrient availability are limiting the ability of the crop to sequester more carbon. This region offers a tremendous possibility of carbon uptake and agricultural yield if this efficiency can be improved. It can be achieved by proper application of fertilizers, selection of a crop type more efficient to capture the solar radiation, and management of soil water content during the crop cycle.

4. Conclusions

In the present work, we have compared the atmospheric CO_2 exchanges of sesame and a reed canary grass, cultivated in the subtropical and boreal climate regimes, respectively using the multi-year EC and supporting meteorological observations. Additionally, we have investigated the effects of climatic variables on the ecosystem–atmosphere CO_2 exchange. Our results show that the carbon uptake by the boreal ecosystem is restricted primarily by the length of the growing season. However, it sequesters more carbon during the short growing season than the subtropical ecosystem due to longer days and high probability of moderate climate compared to the subtropical Indian conditions. It is worth noting here that the carbon uptake by the subtropical ecosystem continues even in the winter when the boreal ecosystem acts as a small but persistent source of atmospheric CO_2. The total carbon uptake by the boreal ecosystem is limited by a short growing season, whereas moisture deficit and poor availability of nutrients in the soil constrain the carbon uptake by the subtropical ecosystem. Our study enables us to compare the aspects of carbon cycles of two different crop types namely oilseed and biofuel. While the former has been a more traditional crop (Alegbejo *et al.* 2003), the latter has recently found widespread popularity due to its immense potential offering of an alternate and renewable source of energy (Jain *et al.* 2010). A comparative analysis of the CO_2 exchange patterns allows us to identify the suitable crop management practices for the oilseed crop such as sesame, a system with high economic value in many parts of the world. In view of the Paris Agreement signed in 2015, such studies carried out for long-term under different climatic conditions are crucial in assessing whether the soils have the ability to address the '4 per 1000' target for soil carbon sequestration.

References

Alegbejo M D, Iwo G A, Abo M E and Idowu A A 2003 Sesame: A potential industrial and export oilseed crop in Nigeria; *J. Sustain. Agric.* **23** 59–76, https://doi.org/10.1300/J064v23n01.

Aubinet M, Grelle A, Ibrom A, Rannik Ü, Moncrieff J, Foken T, Kowalski A S, Martin P H, Berbigier P, Bernhofer C, Clement R, Elbers J, Granier A, Grünwald T, Morgenstern K, Pilegaard K, Rebmann C, Snijders W, Valentini R and Vesala T 1999 Estimates of the annual net carbon and water exchange of forests: The EUROFLUX methodology; *Adv. Ecol. Res.* **30** 113–175, https://doi.org/10.1016/S0065-2504(08)60018-5.

Baldocchi D, Falge E, Gu L, Olson R, Hollinger D, Running S, Anthoni P, Bernhofer C, Davis K, Evans R, Fuentes J, Goldstein A, Katul G, Law B, Lee X, Malhi Y, Meyers T, Munger W, Oechel W, Paw U K T, Pilegaard K, Schmid H P, Valentini R, Verma S, Vesala T, Wilson K and Wofsy S 2001 FLUXNET: A new tool to study the temporal and spatial variability of ecosystem-scale carbon dioxide, water vapor, and energy flux densities; *Bull. Am. Meteorol. Soc.* **82** 2415–2434, https://doi.org/10.1175/1520-0477(2001)082%3c2415:FANTTS%3e2.3.CO;2.

Bhattacharyya P, Neogi S, Roy K S, Dash P K, Tripathi R and Rao K S 2013a Net ecosystem CO_2 exchange and carbon cycling in tropical lowland flooded rice ecosystem; *Nutr. Cycl. Agroecosyst.* **95** 133–144, https://doi.org/10.1007/s10705-013-9553-1.

Bhattacharyya P, Neogi S, Roy K S and Rao K S 2013b Gross primary production, ecosystem respiration and net ecosystem exchange in Asian rice paddy: An eddy covariance-based approach; *Curr. Sci.* **104** 67–75.

Bisht I S, Mahajan R K, Loknathan T R and Agrawal R C 1998 Diversity in Indian sesame collection and stratification of germplasm accessions in different diversity groups; *Genet. Resour. Crop Evol.* **45** 325–335, https://doi.org/10.1023/A:1008652420477.

Boureima S, Oukarroum A, Diouf M, Cisse N and Damme P Van 2012 Screening for drought tolerance in mutant

germplasm of sesame (Sesamum indicum) probing by chlorophyll a fluorescence; *Environ. Exp. Bot.* **81** 37–43, https://doi.org/10.1016/j.envexpbot.2012.02.015.

Burba G 2013 *Eddy Covariance Method for Scientific, Industrial, Agricultural and Regulatory Applications;* Li-Cor Biosciences.

Chatterjee A, Roy A, Chakraborty S, Karipot A K, Sarkar C, Singh S, Ghosh S K, Mitra A and Raha S 2018 Biosphere atmosphere exchange of CO_2, H_2O vapour and energy during spring over a high altitude Himalayan forest at eastern India; *Aerosol Air Qual. Res.* **18** 2704–2719, https://doi.org/10.4209/aaqr.2017.12.0605.

Ciais P, Reichstein M, Viovy N, Granier A, Ogée J, Allard V, Aubinet M, Buchmann N, Bernhofer C, Carrara A, Chevallier F, De Noblet N, Friend A D, Friedlingstein P, Grünwald T, Heinesch B, Keronen P, Knohl A, Krinner G, Loustau D, Manca G, Matteucci G, Miglietta F, Ourcival J M, Papale D, Pilegaard K, Rambal S, Seufert G, Soussana J F, Sanz M J, Schulze E D, Vesala T and Valentini R 2005 Europe-wide reduction in primary productivity caused by the heat and drought in 2003; *Nature* **437** 529–533, https://doi.org/10.1038/nature03972.

Ciais P, Sabine C, Bala G, Bopp L, Brovkin V, Canadell J, Chhabra A, DeFries R, Galloway J, Heimann M, Jones C, Quéré C Le Myneni R B, Piao S and Thornton P 2013 The physical science basis. Contribution of working group I to the fifth assessment report of the intergovernmental panel on climate change; In: *Climate Change 2013: The Physical Science Basis. Contribution of Working Group I to the Fifth Assessment Report of the Intergovernmental Panel on Climate Change*, https://doi.org/10.1017/CBO978110741 5324.015.

Deb Burman P K, Prabha T V Morrison R and Karipot A 2018 A case study of turbulence in the nocturnal boundary layer during the Indian summer monsoon; *Bound.-Layer Meteorol.* **169** 115–138, https://doi.org/10.1007/s10546-018-0364-4.

Deb Burman P K, Sarma D, Morrison R, Karipot A and Chakraborty S 2019 Seasonal variation of evapotranspiration and its effect on the surface energy budget closure at a tropical forest over north-east India; *J. Earth Syst. Sci.* **128** 1–21, https://doi.org/10.1007/s12040-019-1158-x.

Deb Burman P K, Sarma D, Williams M, Karipot A and Chakraborty S 2017 Estimating gross primary productivity of a tropical forest ecosystem over north-east India using LAI and meteorological variables; *J. Earth Syst. Sci.* **126** 1–16, https://doi.org/10.1007/s12040-017-0874-3.

Escobedo J F, Gomes E N, Oliveira A P and Soares J 2009 Modeling hourly and daily fractions of UV, PAR and NIR to global solar radiation under various sky conditions at Botucatu, Brazil; *Appl. Energy* **86** 299–309, https://doi.org/10.1016/j.apenergy.2008.04.013.

Field C B, Barros V R, Dokken D J, Mach K J, Mastrandrea M D, Bilir T E, Chatterjee M, Ebi K L, Estrada Y O, Genova R C, Girma B, Kissel E S, Levy A N, MacCracken S, Mastrandrea P R and White L L 2014 *Climate change 2014 impacts, adaptation and vulnerability: Part A: Global and sectoral aspects: Working group II contribution to the fifth assessment report of the intergovernmental panel on climate change. Climate Change 2014 Impacts, Adaptation and Vulnerability: Part A: Global and Sectoral Aspects*, https://doi.org/10.1017/CBO9781107415379.

Foken T 2008 The energy balance closure problem: An overview; *Ecol. Appl.* **18** 1351–1367, https://doi.org/10.1890/06-0922.1.

Foken T, Göckede M, Mauder M, Mahrt L, Amiro B and Munger W 2004 Post-field data quality control; In: *Handbook of Micrometeorology*, https://doi.org/10.1007/1-4020-2265-4.

Foken T and Wichura B 1996 Tools for quality assessment of surface-based flux measurements; *Agric. For. Meteorol*, https://doi.org/10.1016/0168-1923(95)02248-1.

Fu Y L, Yu G R, Sun X M, Li Y N, Wen X F, Zhang L M, Li Z Q, Zhao L and Hao Y Bin 2006 Depression of net ecosystem CO_2 exchange in semi-arid Leymus chinensis steppe and alpine shrub; *Agric. For. Meteorol.* **137** 234–244, https://doi.org/10.1016/j.agrformet.2006.02.009.

Gelaro R, McCarty W, Suárez M J, Todling R, Molod A, Takacs L, Randles C A, Darmenov A, Bosilovich M G, Reichle R, Wargan K, Coy L, Cullather R, Draper C, Akella S, Buchard V, Conaty A, da Silva A M, Gu W, Kim G K, Koster R, Lucchesi R, Merkova D, Nielsen J E, Partyka G, Pawson S, Putman W, Rienecker M, Schubert S D, Sienkiewicz M and Zhao B 2017 The modern-era retrospective analysis for research and applications, version 2 (MERRA-2); *J. Clim.* **30** 5419–5454, https://doi.org/10.1175/JCLI-D-16-0758.1.

Gnanamoorthy P, Selvam V, Ramasubramanian R, Nagarajan R, Chakraborty S, Deb Burman P K and Karipot A 2019 Diurnal and seasonal patterns of soil CO_2 efflux from the Pichavaram mangroves, India; *Environ. Monit. Assess.* **191** 1–12, https://doi.org/10.1007/s10661-019-7407-2.

Gu S, Tang Y, Du M, Cui X, Kato T, Li Y and Zhao X 2005 Effects of temperature on CO_2 exchange between the atmosphere and an alpine meadow effects of temperature on CO_2 exchange between the atmosphere and an Alpine Meadow; *Phyton* **45** 361–370.

Huxman T E, Turnipseed A A, Sparks J P, Harley P C and Monson R K 2003 Temperature as a control over ecosystem CO_2 fluxes in a high-elevation, subalpine forest; *Oecologia* **134** 537–546, https://doi.org/10.1007/s00442-002-1131-1.

Jain A K, Khanna M, Erickson M and Huang H 2010 An integrated biogeochemical and economic analysis of bioenergy crops in the Midwestern United States; *GCB Bioenergy* **2** 217–234, https://doi.org/10.1111/j.1757-1707.2010.01041.x.

Järveoja J, Laht J, Maddison M, Soosaar K, Ostonen I and Mander Ü 2013 Mitigation of greenhouse gas emissions from an abandoned Baltic peat extraction area by growing reed canary grass: Life-cycle assessment; *Reg. Environ. Change* **13** 781–795, https://doi.org/10.1007/s10113-012-0355-9.

Kaimal J C and Finnigan J J 1994 *Atmospheric Boundary Layer Flows: Their Structure and Measurement*; Oxford University Press, Oxford.

Kandel T P, Elsgaard L and Karki S 2016 Biomass yield and greenhouse gas emissions from a drained fen peatland cultivated with reed canary grass under different harvest and fertilizer regimes; *BioEnergy Res.* **6** 883–895, https://doi.org/10.1007/s12155-013-9316-5.

Karki S, Elsgaard L, Kandel T P and Lærke P E 2015 Full GHG balance of a drained fen peatland cropped to spring barley and reed canary grass using comparative assessment of CO_2 fluxes; *Environ. Monit. Assess.*, https://doi.org/10.1007/s10661-014-4259-7.

Kashiwar S R, Nath T, Kumar D, Kundu M C, Dongarwa U R, Rajput B S, Pandey S K and Dongarwar L N 2018 Evaluation of soil fertility status of Rajiv Gandhi South Campus (Banaras Hindu University), Mirzapur, Uttar Pradesh by using GIS; *Int. J. Curr. Microbiol. Appl. Sci.*, Spec. Issue, pp. 3825–3836.

Kottek M, Grieser J, Beck C, Rudolf B and Rubel F 2006 World map of the Köppen–Geiger climate classification updated; *Meteorol. Zeitschrift* **15** 259–263, https://doi.org/10.1127/0941-2948/2006/0130.

Kumar V and Sharma S N 2011 Comparative potential of phenotypic, ISSR and SSR markers for characterization of sesame (Sesamum indicum L.) varieties from India; *J. Crop Sci. Biotechnol.* **14** 163–171, https://doi.org/10.1007/s12892-010-0102-z.

Lal M, Singh K, Srinivasan G, Rathore L, Naidu D and Tripathi C 1999 Growth and yield responses of soybean in Madhya Pradesh, India to climate variability and change; *Agric. For. Meteorol.* **93** 53–70, https://doi.org/10.1016/S0168-1923(98)00105-1.

Lal M, Singh K K, Rathore L S, Srinivasan G and Saseendran S A 1998 Vulnerability of rice and wheat yields in NW India to future changes in climate; *Agric. For. Meteorol.* **89** 101–114, https://doi.org/10.1016/S0168-1923(97)00064-6.

Lasslop G, Reichstein M, Papale D, Richardson A D, Arneth A, Barr A, Stoy P and Wohlfahrt G 2010 Separation of net ecosystem exchange into assimilation and respiration using a light response curve approach: critical issues and global evaluation; *Glob. Chang. Biol.* **16** 187–208, https://doi.org/10.1111/j.1365-2486.2009.02041.x.

Le Quéré C, Andrew R M, Canadell J G, Sitch S, Ivar Korsbakken J, Peters G P, Manning A C, Boden T A, Tans P P, Houghton R A, Keeling R F, Alin S, Andrews O D, Anthoni P, Barbero L, Bopp L, Chevallier F, Chini L P, Ciais P, Currie K, Delire C, Doney S C, Friedlingstein P, Gkritzalis T, Harris I, Hauck J, Haverd V, Hoppema M, Klein Goldewijk K, Jain A K, Kato E, Kortzinger A, Landschutzer P, Lefevre N, Lenton A, Lienert S, Lombardozzi D, Melton J R, Metzl N, Millero F, Monteiro P M S, Munro D R, Nabel J E M S, Nakaoka S I, O'Brien K, Olsen A, Omar A M, Ono T, Pierrot D, Poulter B, Rodenbeck C, Salisbury J, Schuster U, Schwinger J, Seferian R, Skjelvan I, Stocker B D, Sutton A J, Takahashi T, Tian H, Tilbrook B, Van Der Laan-Luijkx I T, Van Der Werf G R, Viovy N, Walker A P, Wiltshire A J and Zaehle S 2016 Global Carbon Budget 2016; *Earth Syst. Sci. Data* **8** 605–649, https://doi.org/10.5194/essd-8-605-2016.

Lind S E, Shurpali N J, Peltola O, Mammarella I, Hyvönen N, Maljanen M, Räty M, Virkajärvi P and Martikainen P J 2016 Carbon dioxide exchange of a perennial bioenergy crop cultivation on a mineral soil; *Biogeoscience* **13** 1255–1268, https://doi.org/10.5194/bg-13-1255-2016.

Mall R K and Aggarwal P K 2002 Climate change and rice yields in diverse agro-environments of India. I: Evaluation of impact assessment models; *Clim. Change* **52** 315–330, https://doi.org/10.1023/A:1013702105870.

Mammarella I, Peltola O, Nordbo A, Järvi L and Rannik Ü 2016 EddyUH: An advanced software package for eddy covariance flux calculation for a wide range of instrumentation and ecosystems; *Atmos. Meas. Tech. Discuss.*, https://doi.org/10.5194/amt-2015-323.

Mander Ü, Järveoja J, Maddison M, Soosaar K, Aavola R, Ostonen I and Salm J O 2012 Reed canary grass cultivation mitigates greenhouse gas emissions from abandoned peat extraction areas; *GCB Bioenergy* **4** 462–474, https://doi.org/10.1111/j.1757-1707.2011.01138.x.

Matin S and Behera M D 2017 Alarming rise in aridity in the Ganga river basin, India, in past 3.5 decades; *Curr. Sci*, https://doi.org/10.1038/srep20716.

Mauder M, Cuntz M, Drüe C, Graf A, Rebmann C, Schmid H P, Schmidt M and Steinbrecher R 2013 A strategy for quality and uncertainty assessment of long-term eddy-covariance measurements; *Agric. For. Meteorol.* **169** 122–135, https://doi.org/10.1016/j.agrformet.2012.09.006.

McCaughey J H, Pejam M R, Arain M A and Cameron D A 2006 Carbon dioxide and energy fluxes from a boreal mixedwood forest ecosystem in Ontario, Canada; *Agric. For. Meteorol.* **140** 79–96, https://doi.org/10.1016/j.agrformet.2006.08.010.

Mishra V, Aadhar S, Akarsh A, Pai S and Kumar R 2016 On the frequency of the 2015 monsoon season drought in the Indo-Gangetic Plain; *Geophys. Res. Lett.*, https://doi.org/10.1002/2016GL071407.

Moncrieff J B, Massheder J M, de Bruin H, Elbers J, Friborg T, Heusinkveld B, Kabat P, Scott S, Soegaard H and Verhoef A 1997 A system to measure surface fluxes of momentum, sensible heat, water vapour and carbon dioxide; *J. Hydrol.* **188**–**189** 589–611, https://doi.org/10.1016/S0022-1694(96)03194-0.

Moncrieff J, Clement R, Finnigan J and Meyers T 2004 Averaging, detrending and filtering of Eddy covariance time series; In: *Handbook of Micrometeorology*, https://doi.org/10.1007/1-4020-2265-4_2.

Myneni R Y K and Park T 2015 MCD15A3H MODIS/Terra+Aqua Leaf Area Index/FPAR 4-day L4 Global 500m SIN Grid V006; NASA EOSDIS Land Processes DAAC, https://doi.org/10.5067/MODIS/MCD15A3H.006.

Nakai T, Van Der Molen M K, Gash J H C and Kodama Y 2006 Correction of sonic anemometer angle of attack errors; *Agric. For. Meteorol.* **136** 19–30, https://doi.org/10.1016/j.agrformet.2006.01.006.

Nath R, Chakraborty P K and Chakraborty A 2001 Effect of climatic variation on yield of sesame (Sesamum indicum L.) at different dates of sowing; *J. Agron. Crop Sci.* **186** 97–102.

ORNL DAAC 2018 MODIS and VIIRS land products global subsetting and visualization tool; ORNL DAAC, Oak Ridge, Tennessee, USA. Subset obtained for MCD15A3H product at 25.06N, 82.59E, time period: 2014-01-01 to 2016-12-30 and subset size: 0.5×0.5 km, https://doi.org/10.3334/ORNLDAAC/1379.

Pai D S and Bhan S C 2014 *Monsoon 2014. A Report* (Vol. 01). Pune; http://www.imd.gov.in/section/nhac/monsoon_report_2014.pdf.

Papale D, Reichstein M, Aubinet M, Canfora E, Bernhofer C, Kutsch W, Longdoz B, Rambal S, Valentini R, Vesala T and others 2006 Towards a standardized processing of net ecosystem exchange measured with eddy covariance technique: Algorithms and uncertainty estimation; *Biogeoscience* **3** 571–583, https://doi.org/10.5194/bg-3-571-2006.

Patel N R, Dadhwal V K and Saha S K 2011 measurement and scaling of carbon dioxide (CO_2) exchanges in wheat using

flux-tower and remote sensing; *J. Indian Soc. Remote Sens.* **39** 383, https://doi.org/10.1007/s12524-011-0107-1.

Patra P K, Canadell J G, Houghton R A, Piao S L, Oh N H, Ciais P, Manjunath K R, Chhabra A, Wang T, Bhattacharya T, Bousquet P, Hartman J, Ito A, Mayorga E, Niwa Y, Raymond P A, Sarma V V S and Lasco R 2013 The carbon budget of South Asia; *Biogeoscience* **10** 513–527, https://doi.org/10.5194/bg-10-513-2013.

Pinker R and Laszlo I 1992 Global distribution of photosynthetically active radiation as observed from satellites; *J. Clim.*, https://doi.org/10.1175/1520-0442(1992)005%3c0056:GDOPAR%3e2.0.CO;2.

Prabha T V, Khain A, Maheskumar R S, Pandithurai G, Kulkarni J R and Goswami B N 2011 Microphysics of premonsoon and monsoon clouds as seen from in situ measurements during the cloud aerosol interaction and precipitation enhancement experiment (CAIPEEX); *J. Atmos. Sci.* **68** 1882–1901, https://doi.org/10.1175/2011JAS3707.1.

Ramarao M V S, Sanjay J, Krishnan R, Mujumdar M, Bazaz A and Revi A 2018 On observed aridity changes over the semiarid regions of India in a warming climate; *Theor. Appl. Climatol.*, https://doi.org/10.1007/s00704-018-2513-6.

Rannik Ü and Vesala T 1999 Autoregressive filtering versus linear detrending in estimation of fluxes by the eddy covariance method; *Bound.-Layer Meteorol.* **91** 259–280, https://doi.org/10.1023/A:1001840416858.

Reichstein M, Falge E, Baldocchi D, Papale D, Aubinet M, Berbigier P, Bernhofer C, Buchmann N, Gilmanov T, Granier A, Grünwald T, Havránková K, Ilvesniemi H, Janous D, Knohl A, Laurila T, Lohila A, Loustau D, Matteucci G, Meyers T, Miglietta F, Ourcival J M, Pumpanen J, Rambal S, Rotenberg E, Sanz M, Tenhunen J, Seufert G, Vaccari F, Vesala T, Yakir D and Valentini R 2005 On the separation of net ecosystem exchange into assimilation and ecosystem respiration: Review and improved algorithm; *Glob. Change Biol.* **11** 1424–1439, https://doi.org/10.1111/j.1365-2486.2005.001002.x.

Restaino C M, Peterson D L and Littell J 2016 Increased water deficit decreases Douglas fir growth throughout western US forests; *Proc. Nat. Acad. Sci.* **113** 9557–9562, https://doi.org/10.1073/pnas.1602384113.

Rodda S, Thumaty K, Jha C and Dadhwal V 2016 Seasonal variations of carbon dioxide, water vapor and energy fluxes in tropical Indian mangroves; *Forests* **7** 35, https://doi.org/10.3390/f7020035.

Sarma D, Kumar Baruah K, Baruah R, Gogoi N, Bora A, Chakraborty S and Karipot A 2018 Carbon dioxide, water vapour and energy fluxes over a semi-evergreen forest in Assam, northeast India; *J. Earth Syst. Sci.* **127** 94, https://doi.org/10.1007/s12040-018-0993-5.

Sathyanadh A, Prabha T V, Balaji B, Resmi E A and Karipot A 2017 Evaluation of WRF PBL parameterization schemes against direct observations during a dry event over the Ganges valley; *Atmos. Res.* **193** 125–141, https://doi.org/10.1016/j.atmosres.2017.02.016.

Schotanus P, Nieuwstadt F T M and De Bruin H A R 1983 Temperature measurement with a sonic anemometer and its application to heat and moisture fluxes; *Bound.-Layer Meteorol.* **26** 81–93, https://doi.org/10.1007/BF00164332.

Shurpali N J, Hyvönen N P, Huttunen J T, Clement R J, Reichstein M, Nykänen H, Biasi C and Martikainen P J 2009 Cultivation of a perennial grass for bioenergy on a boreal organic soil-carbon sink or source? *GCB Bioenergy* **1** 35–50, https://doi.org/10.1111/j.1757-1707.2009.01003.x.

Shurpali N J, Strandman H, Kilpeläinen A, Huttunen J, Hyvönen N, Biasi C, Kellomäki S and Martikainen P J 2010 Atmospheric impact of bioenergy based on perennial crop (reed canary grass, *Phalaris arundinaceae*, L) Cultivation on a drained boreal organic soil; *GCB Bioenergy* **2** 130–138, https://doi.org/10.1111/j.1757-1707.2010.01048.x.

Solantie, R 2006 Temporal variation of evapotranspiration and growth in Finnish forest in relation to climate; *Geophysica* **42** 35–54.

Wagle P and Kakani V G 2014 Agriculture, ecosystems and environment environmental control of daytime net ecosystem exchange of carbon dioxide in switchgrass; *Agric. Ecosyst. Environ.* **186** 170–177, https://doi.org/10.1016/j.agee.2014.01.028.

Wang B, Jin H, Li Q, Chen D, Zhao L, Tang Y, Kato T and Gu S 2017 Diurnal and seasonal variations in the net ecosystem CO_2 exchange of a pasture in the three-river source region of the Qinghai–Tibetan Plateau; *PLoS ONE* **12** 1–23, https://doi.org/10.1371/journal.pone.0170963.

Wang K and Dickinson R E 2012 A review of global terrestrial evapotranspiration: Observation, modelling, climatology and climatic variability; *Rev. Geophys.* **50** 1–54, https://doi.org/10.1029/2011RG000373.

Watham T, Kushwaha S P, Patel N R and Dadhwal V K 2014 Monitoring of carbon dioxide and water vapour exchange over a young mixed forest plantation using eddy covariance technique; *Curr. Sci.* **107** 858–866.

Watson D J 1947 Comparative physiological studies on the growth of field crops: I. Variation in net assimilation rate and leaf area between species and varieties and within and between years; *Ann. Bot.* **11** 41–76, https://doi.org/10.1093/oxfordjournals.aob.a083148.

Webb E K, Pearman G I and Leuning R 1980 Correction of flux measurements for density effects due to heat and water vapour transfer; *Q. J. R. Meteorol. Soc.* **106** 85–100, https://doi.org/10.1002/qj.49710644707.

Wutzler T, Lucas-Moffat A, Migliavacca M, Knauer J, Sickel K, Sigut L, Menzer O and Reichstein M 2018 Basic and extensible post-processing of eddy covariance flux data with REddyProc; *Biogeosci. Discuss.* **15** 1–39, https://doi.org/10.5194/bg-2018-56.

Corresponding editor: Kavirajan Rajendran